REPORT DOCUMENTATION PAGE

Form Approved OMB No. 0704-0188

AGENCY USE ONLY (Leave blank)	2. REPORT DATE	3. REPORT TYPE AND DATES COVERED
	1997	Final Report

4. TITLE AND SUBTITLE

Studies on Diffraction Efficiency of Optically Addressed Liquid Crystal Spatial Light Modulators for Telescopes with Nonlinear Correction for Distortions

5. FUNDING NUMBERS

F6170896W0318

6. AUTHOR(S)

Dr. Vladimir A. Berenberg

7. PERFORMING ORGANIZATION NAME(S) AND ADDRESS(ES)

Research Institute for Laser Physics
Birjevaya, 12
St. Petersburg 199034
Russia

8. PERFORMING ORGANIZATION REPORT NUMBER

N/A

9. SPONSORING/MONITORING AGENCY NAME(S) AND ADDRESS(ES)

EOARD
PSC 802 BOX 14
FPO 09499-0200

10. SPONSORING/MONITORING AGENCY REPORT NUMBER

SPC 96-4093

11. SUPPLEMENTARY NOTES

12a. DISTRIBUTION/AVAILABILITY STATEMENT

Approved for public release; distribution is unlimited.

12b. DISTRIBUTION CODE

A

13. ABSTRACT (Maximum 200 words)

This report results from a contract tasking Research Institute for Laser Physics as follows: The contractor will investigate experimental and theoretical studies of the factors limiting the diffraction efficiency of spatial light modulators with nematic liquid crystals that are used for correcting wavefront distortions; fabr and test two spatial light modulators with segnetoelectric smectic liquid crystals; perform experimental and theoretical studies of the factors limiting the diffraction efficiency of spatial light modulators with smectic liquid crys that are used for correcting wavefront distortions. Design, fabricate and test spatial light modulators from nematic and segnetoelectric liquid crystals with optimized parameters as determined by steps a) through c).

14. SUBJECT TERMS

Physics, Non-linear Optics, Opto-electronic Materials

15. NUMBER OF PAGES

46

16. PRICE CODE

N/A

17. SECURITY CLASSIFICATION OF REPORT	18. SECURITY CLASSIFICATION OF THIS PAGE	19. SECURITY CLASSIFICATION OF ABSTRACT	20. LIMITATION OF ABSTRACT
UNCLASSIFIED	UNCLASSIFIED	UNCLASSIFIED	UL

Institute for Laser Physics of SC "Vavilov State Optical Institute"

&

Lasers and Optical System, Ltd.

SPC96-4093

STUDIES ON DIFFRACTION EFFICIENCY OF OPTICALLY ADDRESSED LIQUID CRYSTAL SPATIAL LIGHT MODULATORS FOR TELESCOPES WITH NONLINEAR CORRECTION FOR DISTORTIONS

Final Report

Director of the Institute **Prof. Arthur A.Mak**

Principal Investigator **Vladimir A.Berenberg**

St.-Petersburg

1997

Table of content

1. Introduction

This document is the Final Report on the Contract # F61708-96-W0318 between Dr. Vladimir Berenberg as Principal Investigator working through LOS LTD located in St.Petersburg, Russia. The works were made by (alphabetically) V.Berenberg, A.Chaika, A.Leshchev, A.Onokhov, L.Soms, M.Vasiliev, and V.Venediktov.

The Report describes the results of the diffraction efficiency (DE) and the correction for the distortions fidelity studies in the wide spectral range while recording of the dynamic hologram-corrector in the optically addressed liquid crystal spatial light modulators (OA LC SLM). The elements were comprised by either polymer photoconductor (PC) or a-Si_{1-x}:C_x:H (amorphous hydrogenated silicon carbide) PC and either nematic or ferroelectric liquid crystal (NLC and FLC). In the Report there are described the basic optical schemes of the imaging optical systems (OS) with the holographic correction for distortions. Discussed are the types and scale of the distortions usual for such OS, and evaluated are the limitations of the basic parameters of OS, such as field of vision and spectral range of observation, imposed by the application of dynamic holographic corrector on the base of LC SLM. The most prospective variants of the method implementation are discussed.

The results of the reported studies are the basis for the proposals on further elaboration of high efficiency LC SLM for dynamic holographic correction. Two specimens of the OA LC SLM (α-Si_{1-x}:C_x:H PC layer, one with NLC layer and another with FLC layer) are supplied to Customer.

2. Imaging optical systems with the holographic correction for distortions: general provisions

The holographic method of correction for distortions of telescope lens (primary mirror) was proposed and experimentally realized in [1,2]. The hologram-corrector was recorded with the use of coherent radiation; the use of diffraction grating [2,3] on the reconstruction stage for correction for hologram-corrector chromatism made it possible to obtain the corrected images in the comparatively wide spectral range. In these works as well as in later ones [4,5] the static holographic media were used, providing thus the correction only for static distortions. The development of methods providing the record of holograms-correctors in real time scale has revived the interest to this area of optical engineering.

The most obvious areas of application of holographic correction for distortions are the realization of the large scale (primary mirror with the diameter of several meters) telescopes [6] and of the compact transported OS with the comparatively small (~ 1 m) primary mirror for small size and light satellites of the Earth [7].

In the case of application for correction for primary mirror distortions in telescope that images objects extended along the system field of vision and spatially incoherent, it is most reasonable to use the plain (thin) hologram-corrector. To the contrary to the volume (thick, Bragg) holograms such holograms do not reveal angular and spectral selectivity properties. The unique combination of such LC SLM properties as a very high sensitivity, sufficiently fast response time and reversibility, and sufficient resolution and depth of phase modulation, make this medium the most promising for record of thin dynamic holograms. The principle possibility of correction for distortions while imaging of non-coherent source, using the LC SLM, was demonstrated in [8].

2.1. Basic optical schemes of systems with holographic correction for distortions

The record of holographic corrector and correction for distortions in imaging OS implements the so-called schematics of single pass correction [9-11]. Its essence is as follows. The radiation of reference laser (RL) is sent through the optical system. In the plane of LC SLM it interferes with the nondistorted, most usually plain wave of the same RL radiation. Thus the hologram of distortions is recorded. The radiation of the

imaged object passes along the same beamlet and thus is the subject of the same distortions. The diffraction of the latter radiation on the recorded hologram results in reconstruction of non-distorted (corrected) image of the object.

Two variants of such schematics are known. In the first one the RL radiation source is placed nearby the imaged object (Fig.1). In the case of the remote object the radiation from RL and from this object passes practically along one and the same beamlet; such systems are called reciprocal. Main advantage of such a system is the possibility to correct not only for distortions imposed by OS, but to some extent by atmosphere. Obvious disadvantage - the necessity to place the RL nearby the remote object.

Another variant is based on the use of so called nonreciprocal (bypass) OS [12,13]; the generalized schematics of such a system is shown in the Fig.2. In this case it is not necessary to place RL far away from the corrected OS. The radiation of RL, used for corrector recording, is sent via the corrected lens (primary mirror) and the first auxiliary optical system. On the stage of imaging the radiation from the object passes through the same lens (primary mirror), but via the other, second auxiliary optical system and corrector. This variant is compact, but it does not provide a possibility to correct for atmospheric distortions.

Specific feature of such a system is the presence of two auxiliary optical systems, imaging the pupil of the corrected element (say, primary mirror) to the plane of hologram-corrector. The rate of magnification while such an imaging, as well as the spatial carrier frequency of the corrector, determine the field of OS vision and depend on SLM parameters. In the case of LC SLM the magnification rate can be several hundreds to one, while spatial carrier fills in the range from several dozen to several hundred of line pairs per millimeter (lp/mm).

The field of plain holographic corrector vision is limited, in fact, only by the overlap with other orders of diffraction [14]. The measure of this field of vision, the most convenient for our purposes, is in terms of diffraction limited angles on the corrector aperture. This measure is invariant for the overall OS and thus can be recalculated for the object plane of the whole system by the substitution of a corresponding value for the primary mirror. Simple estimations show that in the case of spatial carrier frequency of ~100 lp/mm in the direction of the grating vector and the corrector aperture diameter of several centimeters, the width of field of system vision would be several thousand of diffraction limited angles.

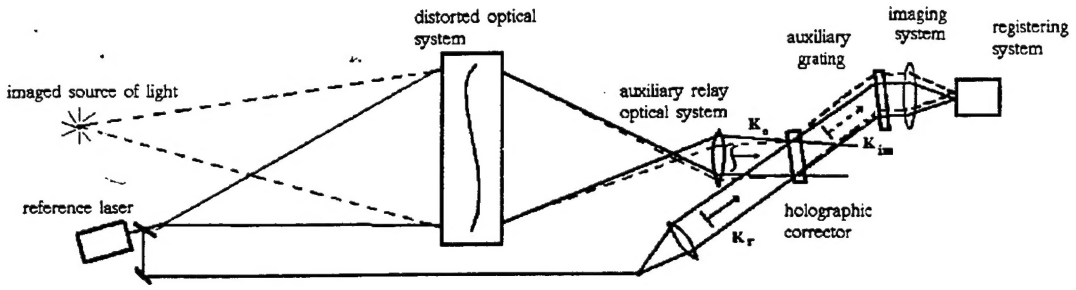

Fig.1. Optical scheme of the reciprocal imaging system with the holographic correction for distortions.

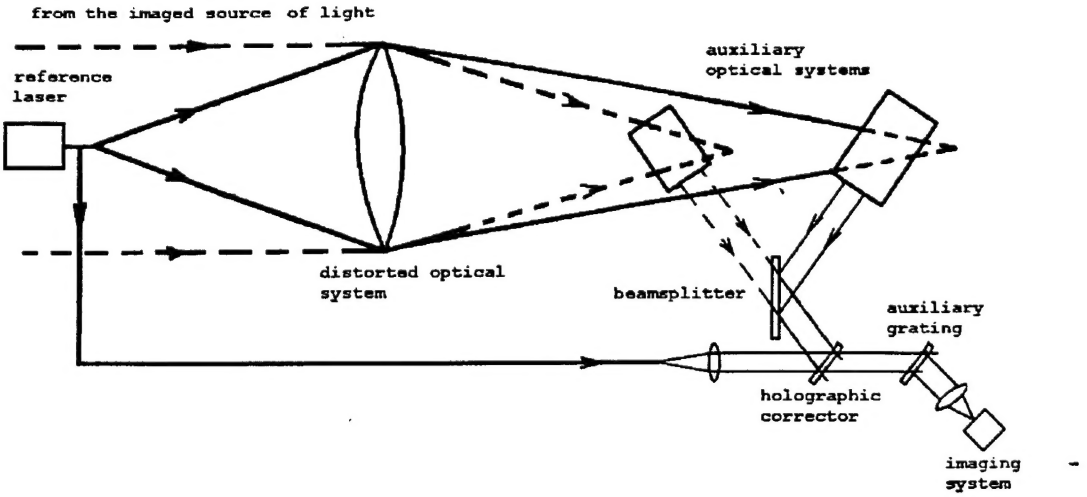

Fig.2. Optical scheme of the nonreciprocal imaging system with the holographic correction for distortions.

2.2. Distortions Types. In OS With Correction And Characteristic Parameters

As we have said already, the holographic correction use is reasonable in the case of large scale OS, using either a poor-quality lightweight monolithic primary mirror or poorly adjusted segmented mirror. The following types of distortions are possible in such systems:

- smooth deformations of wavefronts, usual for OS without correction for distortions, such as coma, astigmatism etc.;
- piston deformations of wavefront, caused by longitudinal shift of mirror segments one with respect to another;
- tilts of wavefront zones, caused by segment tilts;
- combined deformations of wavefronts.

The rate of said deformations could vary across the wide range and depends on the mirror design and technology. Nevertheless, one can make some estimation of maximal rates of distortions. For example, in the case of lightweight segmented mirror with the diameter of 5-8 m, consisting of 5-7 subapertures, the deformation magnitude can be as high as 1-5 μm and general number of defects can be some 20..40 [15].

These figures can be used for evaluation of spatial carrier frequency to be realized in dynamic holographic corrector. The spatial carrier frequency depends also on the corrector diameter - usually some 30..50 mm. So, simple estimation shows that the proper recording of the comparatively smooth relief of phase distortions requires the spatial carrier frequency of at least 10..30 lp/mm.

2.3. Limitations of correction fidelity

There are two classes of limitations of the correction fidelity: the ones which can be eliminated in principle and which are caused by just technical reasons, and those which can not be eliminated in principle and which are caused by the very essence of holographic corrector principle and the nature of hologram record in LC SLM.

The first kind of limitations results from several sources. The first is the difference in the aberrations of the auxiliary systems, used for hologram recording and for image correction (see Fig.2). The others are connected with the optical quality of SLM itself, with light scattering in the OS elements, non-uniform distribution of radiation intensity across the radiation beams, used for corrector recording, etc.

The second class of limitations results from nonlinear character of hologram recording in the LC SLM, leading to some minor delicate effects, which we will not discuss, and of chromatism effects (note that the auxiliary diffraction grating completely compensates for the chromatism only in the case of complete absence of distortions). The role of the latter effects can be easily estimated.

At the reconstruction of the primarily plain wavefront with the phase distortion (shift) $S(r)$, encoded in hologram at the wavelength of λ, at the wavelength $\lambda+\delta\lambda$, the residual error is observed - $\delta S(r)$ - that is determined by the relationship:

$$\delta S = S \cdot \delta\lambda/\lambda$$

So in the case of imaging of non-monochrome objects the distortions at the shifted wavelengths are not corrected completely, but just dumped n times:

$$n = S/\delta S = \lambda/\delta\lambda$$

Numerous applications require the dumping coefficient of about 10 times, which can result in significant increase of image quality. One can see that for the visible range (450..650 nm) of spectrum this dumping rate can be realized within the spectral band of ~ 50 nm width.

This brief analysis of some special features of OS with holographic correction for distortions makes it possible to determine the adequate conditions of the experimental study of LC SLM parameters.

3. Experimental study of diffraction efficiency and correction for distortions fidelity in wide spectral range

The subjects of the study were spatial light modulators (SLM), comprised by polymer photoconductor (PC) or α-Si_{1-x}:C_x:H photoconductor, and either nematic or ferroelectric liquid crystal (LC). The reasons for this choice were as follows. The polymer PC provides the highest available diffraction efficiency (DE) among all layers when the spatial frequency of the hologram exceeds ~ 100 lp/mm. At the same time the parameters of the α–Si_{1-x}:C_x:H PC layer can be varied across the wide range and thus the proper tradeoff between the spatial resolution and reversibility can be chosen.

3.1. Experimental setup

In the Fig.3 is shown the scheme of the experimental setup. The imaged thermal source of radiation, placed in the infinity, was simulated by the tungsten wire of lamp 1 (in the further experiments – by the bar test table), mounted in the focal plane of the lens 2.This object was imaged by the lens telescope (1:1), comprised by the primary lens 3 and the eye-piece 4. The angular size of the imaged object was 0.01 rad. The corrector unit comprised the LC SLM 5 for the dynamic hologram recording, the static transparent phase grating 6, compensating for the dynamic hologram chromatism and the auxiliary elements for the dynamic hologram recording.

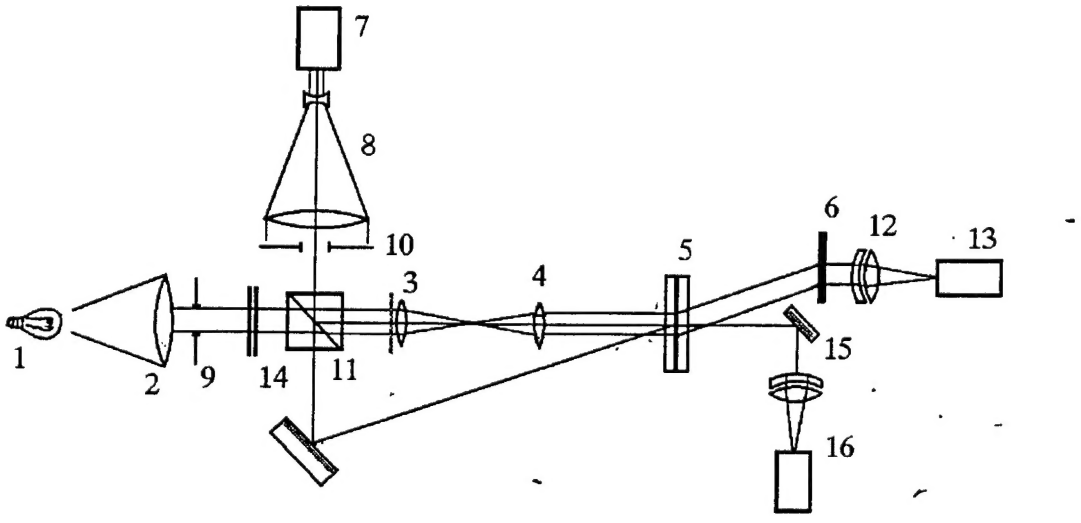

Fig.3. Experimental setup.

The dynamic hologram - corrector was recorded by the pulsed radiation (pulse duration 20-30 ns) of the laser 7 with the wavelength 0.54 μm as the interference pattern of the plain reference wave and the signal wave distorted by the telescope lens. The energies of the signal and reference waves related as 1 : 0.7. Spatial homogeneity of the recording radiation was improved by the use of the auxiliary beam expanding telescope 8 (magnification 1:10). The diameter of the working zone of SLM was determined by the apertures 9 and 10 and equaled 15 mm. The beam splitting cube 11 separated the reference and signal beams and at the same time combined at the telescope input the signal beam of laser radiation and the radiation from the imaged thermal object.

The dynamic hologram - corrector 5 was mounted in the plane where the eyepiece 4 imaged the pupil of the lens 3. The spatial carrier frequency of the dynamic hologram was chosen as the result of tradeoff between the sufficiently high DE and the lack of overlap of the test-object images in different diffraction orders. It equaled 95 lp/mm, chosen to be exactly equal to the spatial frequency of the static holographic grating 6.

After diffraction on the grating 6 the radiation from the thermal source was collected by the lens 12 and focused to the CCD-matrix 13 of the registration system. The spectral range, used for the object imaging, was varied by the colored filters 14. We have used the filters made of standard colored glasses (the spectral characteristics of the filters transparency are shown in the Fig.4), and the band interference filter with the width of the transparency band 10 nm centered at 0.53 μm. The mirror 15 sent the zero diffraction order of the radiation from the thermal source to the auxiliary registration system 16 controlling the non-corrected image quality.

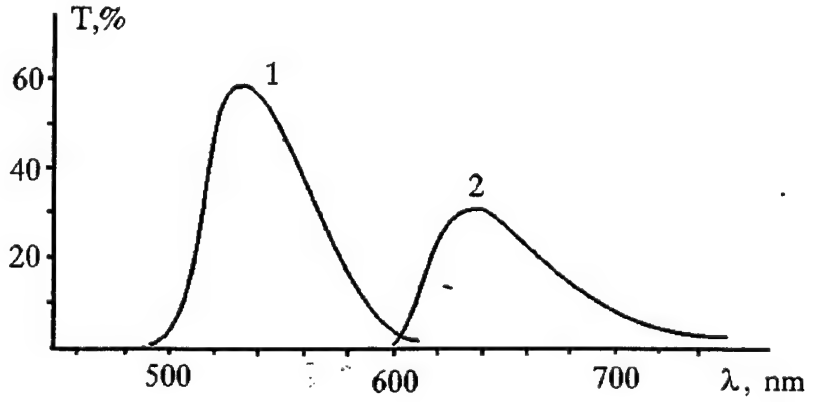

Fig.4. Spectral dependence of the colored filters transparency.

1 – filters ЖС-18 + СЗС-22; 2 – КС-10+СЗС-23

In the experiments where the absolute value of DE of the dynamic grating, recorded by two plain waves, and its temporal behavior were studied, the tungsten lamp 1 was replaced by the monochrome light source; either He-Ne laser (0.63 μm) or light emitting diode (0.82 μm) were used. The CCD-matrix 13 was replaced by the photosensitive diode, whose signal was recorded by the oscilloscope. The diffraction grating 6 was not used in these measurements. The photoelectric sensor was used for the recording radiation energy measurement.

3.2. Diffraction efficiency of SLM with polymer PC

The diffraction efficiency of the holograms, recorded in the OA LC SLM using the organic polymer PC and nematic LC [16,17] in the range of spatial frequencies of more than 100 lp/mm, can be as high as 20-35% [17,18]. Such high diffraction efficiency is available because of the low mobility of charge carriers in the polymer PC [17]. Low mobility, at the same time, results in rather low reversibility of such SLM - just several Hz or even less. Some improvement of the situation can be achieved by the recording schematics improvement, namely, by recording of sequential dynamic holograms in various zones of large SLM; note, that polymer PC is rather cheap and large size elements are easily available. In [19,20] there was shown the possibility to use the SLM of such a kind for the correction for the distortions in the monochrome radiation.

The SLMs, tested in our experiments, were realized as the sandwich structure, whose layers were positioned between two glass substrata (diameter 35 mm). The element cut is shown in the Fig.5. The thickness of the polyimide PC layer was ~ 1.2-1.4 μm. Optical quality of the element across the zone of 15 mm width was not worse than λ/4.

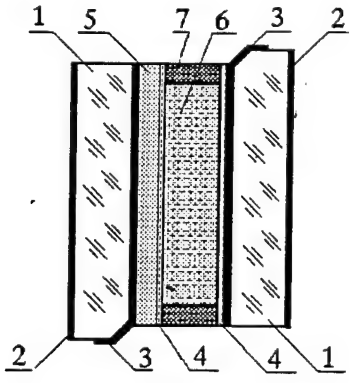

Fig.5. SLM design: 1 - glass substrata, 2 - AR coating, 3 - transparent electrode, 4 - alignment layer, 5 - PC layer, 6 - LC layer, 7 -spacer.

3.2.1. SLM with polymer PC and nematic LC

We have studied two SLM specimens: SLM 1 with the nematic LC layer thickness 4 μm and SLM 2 with the NLC layer thickness of 6 μm. The rate of optical anisotropy of NLC at 0.63 μm wavelength equaled 0.16 and the rate of dielectric anisotropy - 9.9. We have used S-effect for the refraction index modulation [22]. The primary orientation of the molecules in the NLC layer was nearly planar.

The SLM of the discussed kind can be fed by either pulsed or CW voltage and can be used for hologram recording by either pulsed or CW radiation. The preliminary studies have shown that the best mode of the element use for the dynamic hologram recording implements the combination of short (several dozen μsec or less) pulses of radiation and the rectangular shaped voltage pulses. Such a mode of action usually provides the highest values of DE. Non-durable voltage action to a large extent eliminates the negative influence of the electrolyzis of admixtures to LC.

In this case the SLM action is based on transient processes in LC and PC. SLM is fed by the rectangular voltage pulse. Its duration and amplitude are chosen so as to provide, for instance, the highest peak value of DE. The relationship of the resistance of PC and LC provides the sufficient value of the voltage, applied to LC layer so as to induce the homeotrope orientation of its molecules instead of the primary planar orientation. Hence during the voltage pulse the reorientation of LC molecules is impossible. The recording radiation pulse is delayed in several milliseconds with respect to the beginning of the feeding voltage pulse. Radiation results in generation of charge carriers. The electric filed moves the induced free carriers to the semiconductor layer boundaries, screening thus its internal zone. Thus the image relief is imprinted in PC layer, which is stored until the transient processes take place. The storage time is as large, as small is the rate of thermal generation of free charge carriers. On this stage the element resolution is limited by the diffuse washing out of the charge carriers distribution relief. However, the sufficiently intense electric filed in semiconductor dumps the diffuse washing out [21]. Establishing of the complete screening of the semiconductor interior layer results in the resolution degradation.

After switching off the voltage pulse, the polarization field switches on the move of stored charge carries inside the semiconductor layer, where they recombine. The voltage, applied to LC layer, is reducing, and thus the molecules of LC are

relaxing to the primary planar orientation. The parameters of this relaxation process depend on specific structure of the stored image relief.

Of course, the given description of the image recording and conversion in SLM is quite qualitative; numerous features, special for the polymer PC, were just omitted. These are, in particular, the specific dependencies of the charge carriers generation quantum efficiency and their mobility vs. electric field tension as well as the presence of traps and sticking levels, the monopolar character of conductivity etc. [16,17].

The dependencies of the phase shift (retardation) in SLM vs. time and energy fluency of recording radiation were determined in the auxiliary experiment. The SLM was mounted between the crossed polarizers and the system transparency was measured at He-Ne laser wavelength of 0.63 μm. The illumination was induced by the pulses (duration 20-30 ns) of laser radiation at 0.54 μm with the uniform intensity distribution across the beam section. Beam diameter equaled 1 cm. Feeding voltage (50V) pulse duration was ~2 s.

In the Fig.6-8 the results are shown of measurements and processing of experimental data for SLM 1. In the Fig.6 the dependencies are shown of SLM transparency vs. time for several values of recording energy fluency E. In the Fig.7 and Fig.8, also for several values of E, the dependencies are shown of the phase retardation in the element vs. time and differential phase shift with and without SLM irradiation.

These data indicate the possibility to realize in SLM, while recording the dynamic holographic gratings, the nearly maximal possible for the given geometry phase retardation at the recording radiation energy fluency of 150..200 $\mu J/cm^2$. Note that increase of spatial frequency will result in lower amplitude of such holographic gratings due to the transverse washing out of the charge at the boundary PC-LC, due to the elastic deformation of LC and to some other reasons [22]. Seemingly, the numerical account of all this factors influence onto DE value and onto the correction fidelity is hardly possible now and thus the experimental approach is the most promising.

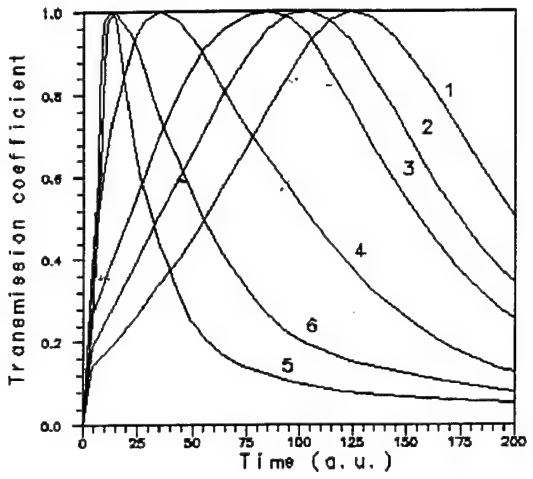

Fig.6. Temporal behavior of SLM transparency in crossed polarizers for E = 0 (1), 150 (2), 230 (3), 330 (4), 450 (5) and 530 (6) μJ/cm^2; 1 unit of time = 6.4 ms.

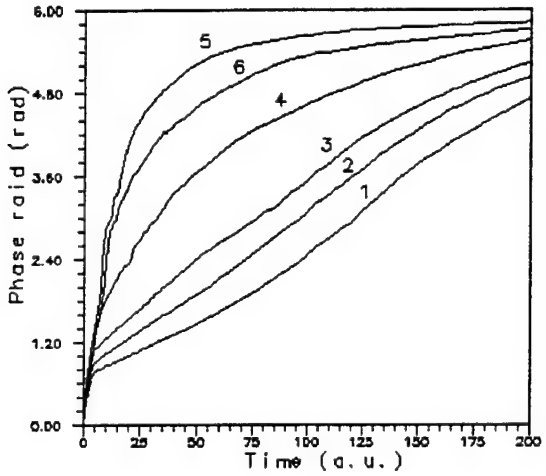

Fig.7. Temporal behavior of phase retardation in SLM for E = 0 (1), 150 (2), 230 (3), 330 (4), 450 (5) and 530 (6) μJ/cm^2; 1 unit of time = 6.4 ms.

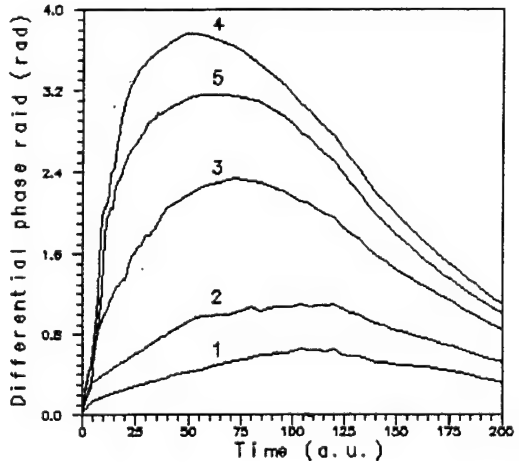

Fig.7. Temporal behavior of differential phase retardation in SLM for E = 0 (1), 150 (2), 230 (3), 330 (4), 450 (5) and 530 (6) μJ/cm^2; 1 unit of time = 6.4 ms.

The absolute value of DE and its temporal behavior were measured at the setup, described in the end of it.3.1. The holograms were read out by He-Ne laser radiation; note that PC was not sensitive to this radiation. The reading-out radiation was polarized parallel to the director. The grating vector was either parallel or perpendicular to the director. The recording radiation pulse was delayed in several milliseconds with respect to the forward front of feeding voltage pulse. The increase of the said delay over some 1-2 ms did not result in any extra modification of DE value and in its temporal behavior. The response was observed after the end of the voltage pulse. Thus the control of this pulse duration provided the control of the delay of the response with respect to the recording radiation pulse. This delay could have been tuned in the range from several dozen milliseconds to several dozen seconds. The results were as follows:

- We have determined the existence of the optimal recording energy fluency E (the integral energy of reference and signal waves) and of the optimal feeding pulse amplitude, polarity and duration; their optimal combination provided the highest peak value of DE. It can be seen from the Fig.9-12, presenting the results for the gratings (spatial frequency 95 lp/mm) recorded in SLM 1. In the Fig.9 are shown the dependencies (arbitrary units) of DE temporal behavior for feeding voltage pulses with the amplitude 50 V and various duration. In the Fig.10 are shown the dependencies of DE vs. E for various amplitudes of feeding pulse at optimal voltage pulse duration. Temporal behavior of DE for several values of E is shown in the Fig.11. Fig.12 illustrates the influence of the feeding voltage pulse polarity (+/- 50V) onto the DE value and behavior.
- Peak DE was measured for the gratings with different spatial frequency. For SLM1, the peak value of DE for the frequency of 100 lp/mm was 20.25%, for 150 lp/mm 6 - 9%, for 200 lp/mm - 2% and for 300 lp/mm - 1%. For SLM2, at the spatial frequency 52 lp/mm the DE peak value equaled 35..40% and for 100 lp/mm 18 - 23%. Note that higher values of DE (20% and more) are available in principle for this kind of SLM at spatial frequencies of 200 - 300 lp/mm [17,18]. However, it needs better mutual matching of LC and PC parameters, which can be obtained only as a result of significant additional experimental testing and elaboration.

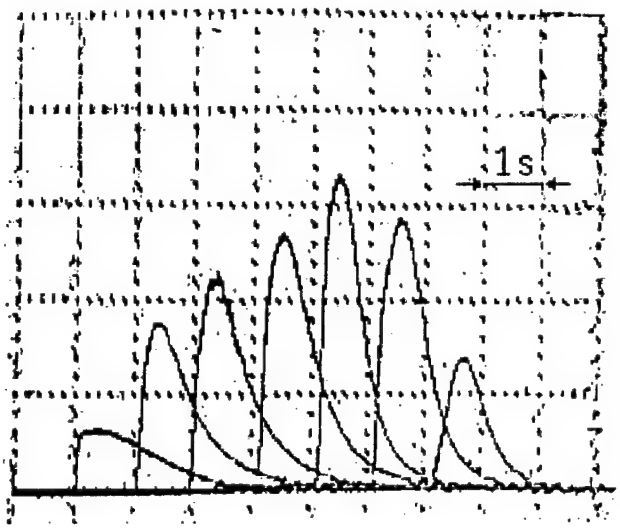

Fig.9. Temporal behavior of DE for feeding pulse duration 1..7 seconds; E = 200 $\mu J/cm^2$.

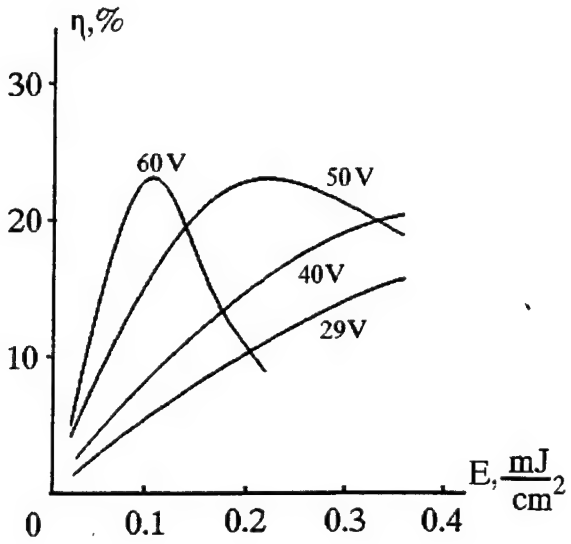

Fig.10. Dependence of peak value of DE vs. recording energy fluency for various amplitude of feeding voltage pulse.

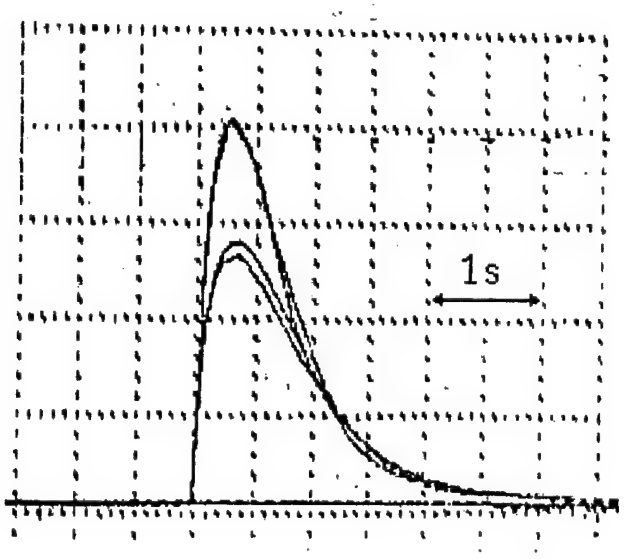

Fig.11. Temporal behavior of DE for the recording energy fluency of 150, 160, 190 and 210 $\mu J/cm^2$.

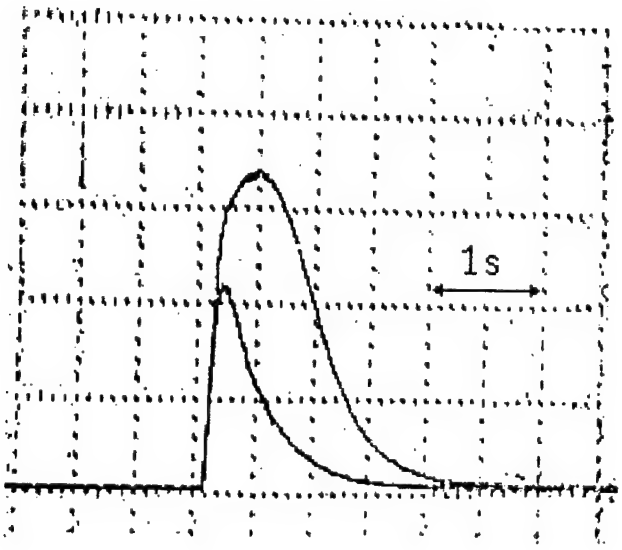

Fig.12. Temporal behavior of DE for feeding voltage pulses of different polarity.

3.2.2. SLM with polymer PC and ferroelectric LC.

One specimen of SLM with ferroelectric LC was fabricated for these studies. The LC compound consisted of non-chiral smectic C LC with chiral admixtures. Spontaneous polarization of FLC equaled 150..200 nC/cm^2, its helicon step was 0.2 μm and the tilt angle of the director θ_0 in smectic layer was 40 degrees. The thickness of FLC layer d was 5 μm. The value of d was significantly much more than helicon step; hence the refraction index modulation was obtained via the effect of the Deformed Helix Ferroelectric, DHF-effect [23,24]. The DHF-effect was chosen due its advantages [23,26] in comparison with the other possible effect in FLC, viz. Clark-Lagerwall effect [25]:

- This effect is less sensitive to the FLC layer thickness variation nearby its optimal value. The effective birefringence for DHF-effect is ~ 1.5 times smaller than that for Clark-Lagerwall effect.
- Long time optical storage is possible for the voltage values nearby the de-twist voltage. The storage time depends on viscosity and elasticity coefficients, on the helicon step, and also of the specific method of electrodes surface processing. This time can be varied from several dozen milliseconds to several dozen seconds. DHF-effect also provides the natural gray scale.
- FLC can be aligned by the means applicable to the nematic crystals.

It was shown earlier (see the results of the Contract between the Institute for Laser Physics, SC Vavilov State Optical Institute", St.-Petersburg, Russia and Company BDI Inc., USA, which has served as the basis for the reported work start) that, in the case of Clark-Lagerwall effect, the maximal value of DE does not depend on the polarization of the reading out radiation and can be described by the relationship:

$$\eta_{max} = [2/\pi \sin(2\theta_0) \sin(\Gamma/2)]^2,$$

Here Γ is the phase retardation in FLC at the wavelength of reading radiation. Further increase of the tilt angle θ_0 in comparison with the realized 40° is hardly practically reasonable. It is obvious that in the case of DHF-effect the phase retardation can be also described by the same formula. However, the dependence of the phase retardation Γ vs. FLC layer thickness d and vs. optical anisotropy of LC for DHF-effect is more complicated than for Clark-Lagerwall effect. One can see from the formula that the maximal value of DE is realized when $\sin^2(\Gamma/2) = 1$.

The same setup, described at the end of Sec.3.1, was used for measuring of DE absolute value and its temporal behavior using the He-Ne laser radiation. SLM was controlled by the combination of CW voltage with the sequence of rectangular shaped voltage pulses. The pulses of positive polarity with the amplitude V_{pp} and controlled duration were superposed onto the negative bias V_b. In the course of our experiments we have varied the polarization of reading radiation, grating vector orientation with respect to the smectic layers normal, the recording energy fluency E, the value of peak-to-peak amplitude of controlling voltage V_{pp}, the bias V_b, the duration of the rectangular shaped pulses, and the delay of the recording radiation pulse with respect to the forward front of the rectangular shaped pulse. The results were as follows:

- DE value only slightly depends on the reading-out light polarization orientation with respect to the grating vector. The value of DE is maximal when the grating vector is parallel to the direction normal to the smectic layers. The tilt of the grating vector results in the graduate reduce of DE, reaching its minimum when the said vector and normal are orthogonal to each other. Seemingly, this dependence results from the flex-electric polarization of FLC, which, in turn, is caused first of all by variation of the polar angle of LC molecules with respect to smectic layers, induced by the electric field [23,27].
- DE absolute value and temporal behavior to a large extent depend on relationship between V_{pp} and V_b and on their absolute value, on the recording energy fluency E and on recording pulse delay τ_0. The simplest dependence is that on τ_0 value. This delay increase up to some 10-20 ms results in shortening of the response pulse forward front. Further increase of the delay τ_0 practically does not cause any variation in DE value and behavior. For any recording energy fluency E the maximal DE was observed when V_{pp} was equal 40-50 V. At the same time for each specific value of E there exists some value of bias V_b, providing maximal peak value of DE. For some values of V_b there was realized the effect of optical memory. The above said is illustrated by the curves, shown in the Fig.13-17, registered when the grating with the spatial frequency 95 lp/mm was recorded. The Fig.13-16 represent the transformation of DE response temporal behavior with variation of the bias V_b for fixed V_{pp} = 40 B. The duration of rectangular voltage pulses was 3 seconds, their repetition rate 0.1 Hz and τ_0 - 2 ms. Modification of the response temporal behavior when the delay time was increased up to 1 second

is illustrated by the Fig.17. The optical memory regime corresponds to Fig.16,17 – the diffraction response lasts until the driving voltage V_{pp} exists

- It was determined that, in comparison with the SLM using NLC, those with FLC provide higher reversibility of diffraction grating record without DE decrease. For the record repetition rate of 1 Hz the each sequential recorded grating did not reveal any residual noise from the preceding grating (Fig.18). The residual light modulation, which can be seen at the oscillograms, is caused first of all by radiation scattering on domains, induced by the voltage polarity switching. The possibility to renew the gratings with the repetition rate of 1 Hz is illustrated by the Fig.19. Response amplitude variation from pulse to pulse is correlated with the recording pulses energy variation. The presence of spontaneous polarization in FLC is, probably, responsible for dumping of the processes of the slow relaxation of the charge relief in polyimide. The intense internal fields in FLC layer may cause, after the switching, an additional driving voltage applied to PC thus helping the washing out the charge relief[23].
- We have measured the peak values of DE of gratings with arbitrary spatial frequency. For the spatial frequency of 52 lp/mm the peak value of DE equaled 17-19%, and for 95 lp/mm - 16-18%. The comparatively "low" value of DE is resulted, most probably, from non-optimal FLC layer thickness. Note the very small reduce of DE value while increase of spatial frequency of the grating from ~ 50 to ~ 100 lp/mm. In the Fig.20 are shown the dependencies of the peak DE values vs. recording energy fluency for two values of spatial frequency. These dependencies were recorded for V_{pp} = 40 V. The bias V_b was chosen so as to provide the highest possible value of DE. For the spatial frequency of 52 lp/mm the optimal voltage was V_b = 23 V, while for 95 lp/mm - V_b = 21 V. Voltage pulse duration was equal 1s, pulse repetition rate - 0.1Hz and τ_0 - 2ms.

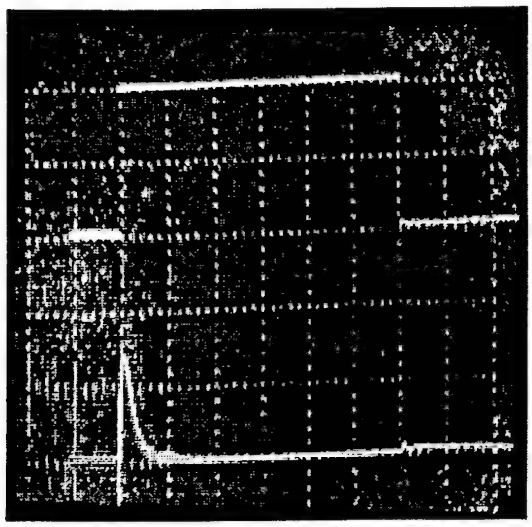

Fig.13. Temporal behavior of DE (lower curve) for V_b = 13 V; upper curve - feeding voltage pulse, single unit = 0.5 sec.

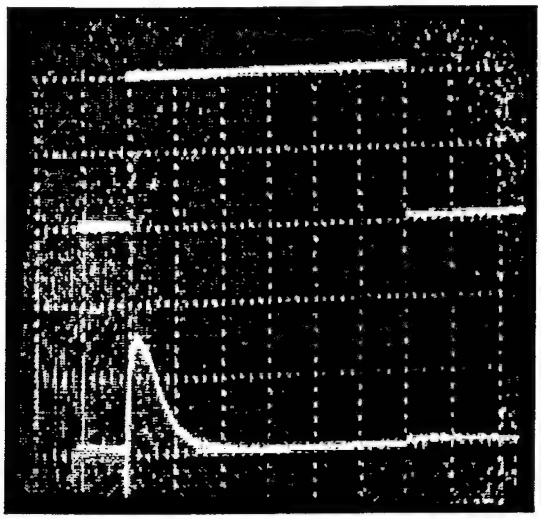

Fig.14. Temporal behavior of DE (lower curve) for V_b = 16 V; upper curve - feeding voltage pulse, single unit = 0.5 sec.

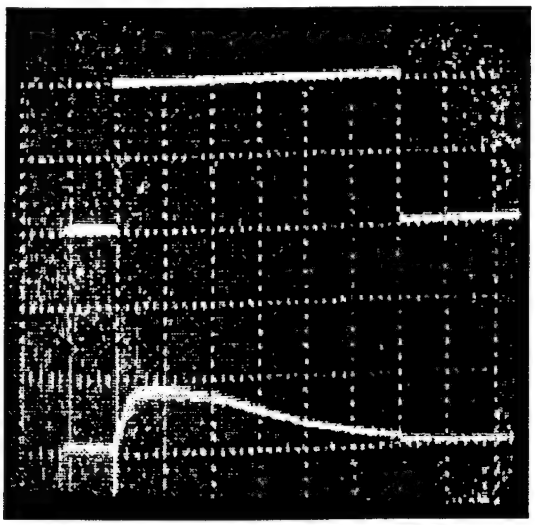

Fig.15. Temporal behavior of DE (lower curve) for V_b = 24 V; upper curve - feeding voltage pulse, single unit = 0.5 sec.

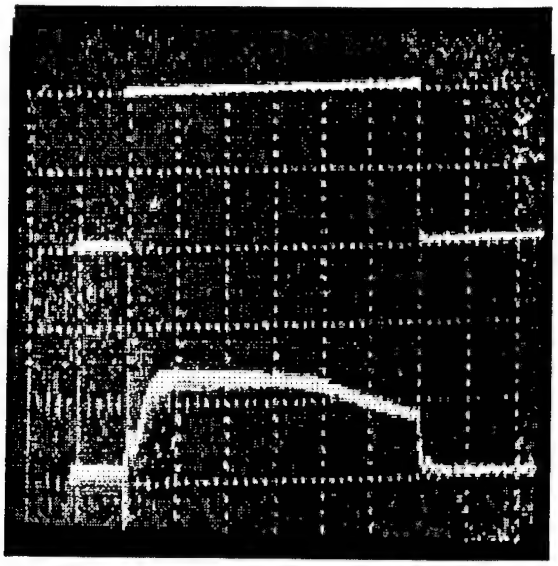

Fig.16. Temporal behavior of DE (lower curve) for V_b = 25 V; upper curve - feeding voltage pulse, single unit = 0.5 sec.

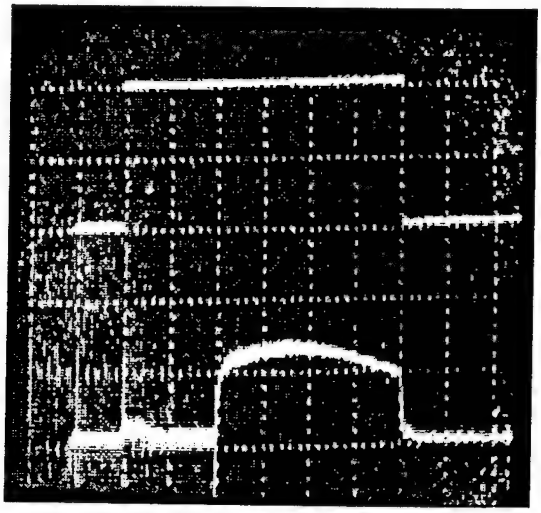

Fig.17. Temporal behavior of DE (lower curve) for V_b = 25 V and recording pulse delay in 1 second; upper curve - feeding voltage pulse, single unit = 0.5 sec.

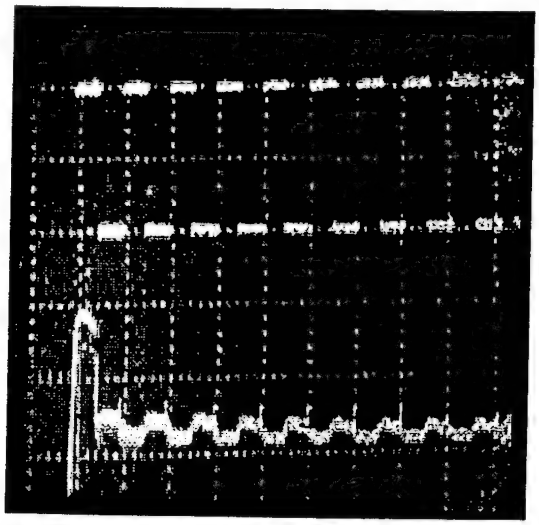

Fig.18. SLM response to single recording pulse (lower curve); upper curve - feeding voltage pulses, single unit = 1 sec.

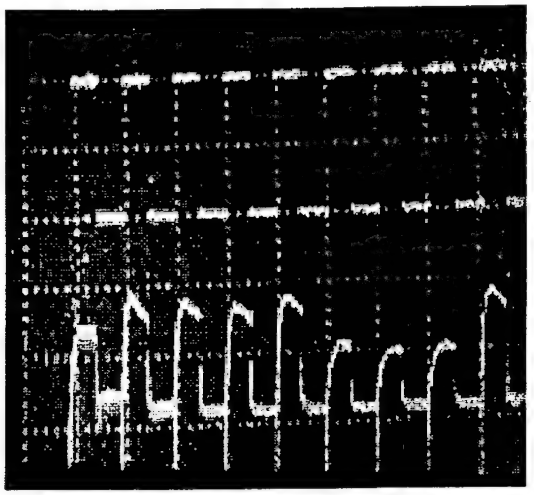

Fig.18. SLM response to repetitively (1 Hz) recorded grating (lower curve); upper curve - feeding voltage pulses, single unit = 1 sec.

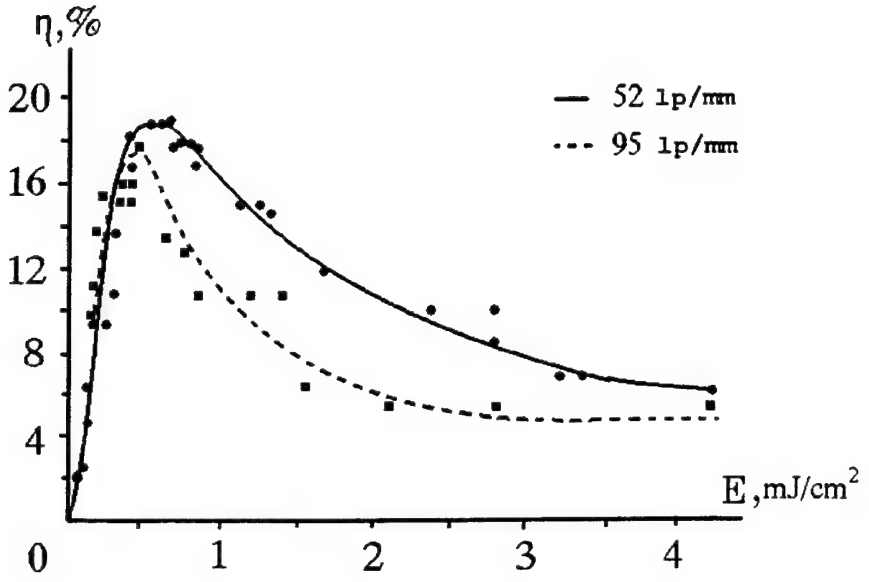

Fig.20. DE dependence vs. recording radiation energy fluency for gratings with various spatial frequency

3.3. Diffraction efficiency of SLM with α-Si:C:H PC

Until now the best response time in OA LC SLM was realized with the use of PC, made of the amorphous hydrated silicon (α-Si:H) and p-i-n structures on this base [28-30]. However, the comparatively high dark conductivity of this medium puts under the question realization of high DE values, close to the extreme possible (30-40%), for the spatial frequencies of 50-100 lp/mm. In addition, transparency of α-Si:H PC in the visible range of spectrum is low, resulting thus in radiation energy losses in the transparent SLM elements.

The use of elements with α-Si_{1-x}:C_x:H PC [31] makes it possible to improve spatial resolution of SLM, preserving yet high reversibility. According the results of our studies the variation of Si and C content in composition provides variation of the dark conductivity, spectral and optical properties of α-Si:C:H layers across the wide range [32,33]. It can be seen from the curves in the Fig.21-23.

The layers of the material were obtained by means of radio frequency dissociation of silane in the multichamber setup. The carbon concentration has been varied by means of control of flows of the methane-containing and silane-containing gaseous mixtures. One can see from the presented curves that the carbon content increase results in reduce of conductivity and refraction index of α-Si:C:H layers. The zones' gap in layer is thus increased, resulting in the reduce of the absorption in red spectral range. Of course, the reduce of dark conductivity results in smaller light sensitivity with that of a-Si:H PC layer; however, its absolute value is yet rather high. In [34,35] there was shown the possibility to make up the p-i-n structure of α-Si:C:H, which is necessary for the SLM element realization. In [34] the SLM with FLC and such PC layer was realized. Its resolution was 70 lp/mm with the reversibility of 1.5 kHz. The SLM of such a kind with NLC layer, realized in [35], revealed the resolution of 50 lp/mm with the reversibility of 50 Hz.

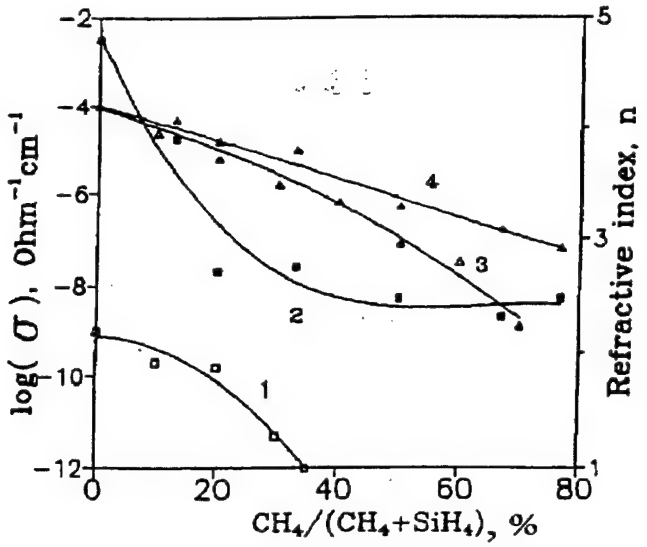

Fig.21. Conductivity (curves 1,2) and refraction index (curves 3,4) of α-Si_{1-x}:C_x:H film vs. C content; 1, 3 - undoped film, 2, 4 - phosphorus doped film.

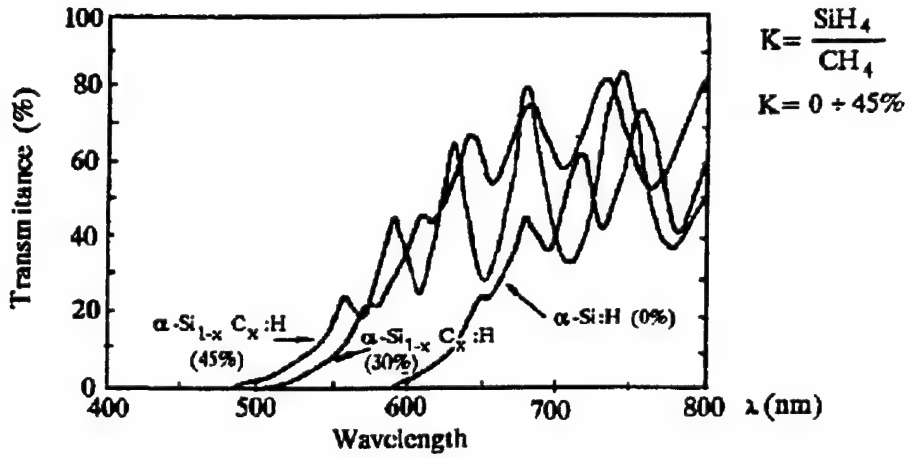

Fig.22. Spectral transparency of α-Si_{1-x}:C_x:H layer with the thickness of 1.2 μm.

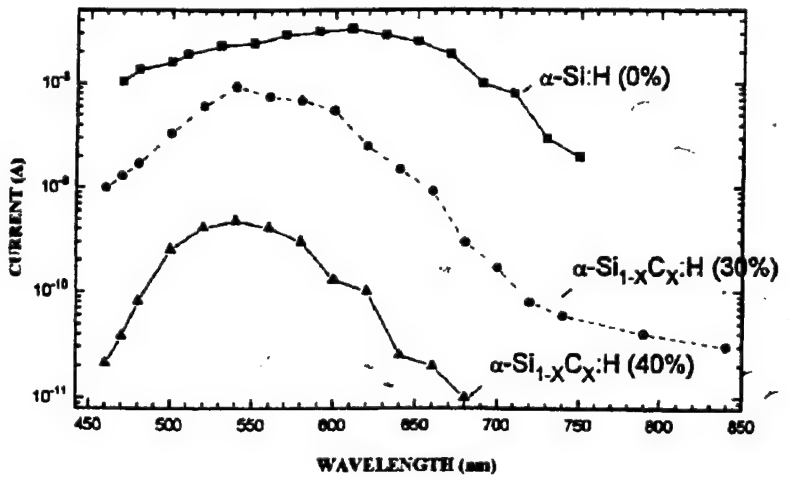

Fig.23. Spectral dependence of photo current of α-Si_{1-x}:C_x:H films.

3.3.1. SLM with α-Si:C:H PC and nematic LC

We have studied two specimens of SLM with the NLC layer thickness 3.5 μm (SLM 1) and 4 μm (SLM 2). The rate of optical anisotropy of NLC at 0.63 μm wavelength equaled 0.16 and the rate of dielectric anisotropy - 9.9. We have used S-effect for the refraction index modulation. The primary orientation of the molecules in the NLC layer was nearly planar. The thickness of α-Si_{1-x}:C_x:H PC layer was approximately 1.2 μm. The ratio of Si and C content corresponded to K = 33 %.

DE absolute value and its temporal behavior were measured at the setup described at the end of Sec.3.1. In this case the ratio of the signal beam energy to that of the referent one was slightly decreased down to 1:0.9. This kind of PC is sensitive to the radiation of He-Ne laser, hence in this series of experiments we have used the radiation from the light emitting diode with the wavelength 0.82 μm. The reading out radiation polarization was parallel to the director. The grating vector was either parallel or orthogonal to the director.

According to the results of our studies the best SLM performance is realized when it is controlled by the repetitive rectangular pulses of voltage, superposed onto the CW voltage shift (bias) (see also it.3.2.2). The response signal was observed after finishing of the voltage pulse. The qualitative character of DE value and temporal behavior dependencies on the magnitude, polarity and duration of the voltage pulses, of the recording energy fluency and on the recording radiation pulse delay with respect to the voltage pulse forward front was similar to that in SLM with NLC and polymer PC (see it.3.2.1). This similarity indicates the similar character of the diffraction grating recording and processing in these two cases. Of course, these two kinds devices have revealed some differences, first of all in the modes of SLM control, the voltage pulse duration providing the maximal DE, and in temporal behavior of DE. These differences were as follows:

- Peak value of DE was maximal for the feeding voltage pulses of 30-40 ms, amplitude V_{pp} = 60 V and bias V_b = 5 V.
- Temporal dependence of DE looked like practically symmetrical waveform with the duration of ~ 0.5 sec at the level of 0.1 of maximal energy. The reversibility of grating record without peak DE value drop was some 3-5 Hz. However, already for the repetition rate of 3.3 Hz we have observed the incomplete washing out of

the preceding grating. This can lead to a degradation of properties of holographic correctors using such SLMs.

The maximal value of DE for the grating with the spatial frequency of 52 lp/mm in SLM 1 was 20-21 %. It was realized for V_{pp} = 60 V and V_b = 5 V, voltage pulse duration of 30 ms and τ_0 = 1 ms. Positive polarity of the voltage pulses was applied to the photoconductor layer. In the Fig.24 is shown the dependence of DE vs. E for SLM1, for the pulse repetition rate of 1 Hz. Grating vector was parallel to the director. Seemingly, the smaller DE peak value in the discussed kind of SLM, in comparison with the polymer PC SLM, is determined by the much (1-2 orders of magnitude) higher dark conductivity of α-Si:C:H. For SLM2, DE was ~1.5 times smaller; the possible reason is some variation of properties of two α-Si:C:H PC layers due to yet non-mastered production technology.

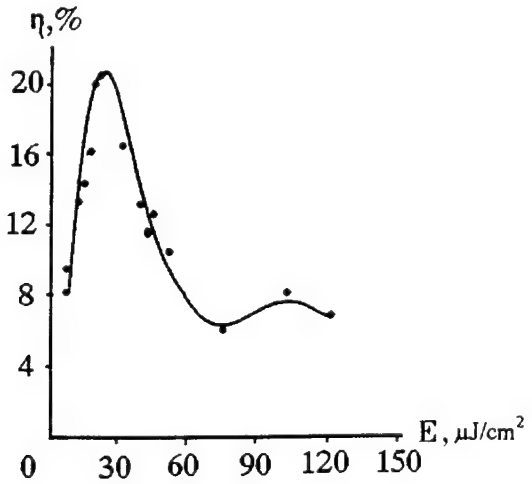

Fig.24. Grating diffraction efficiency vs. recording radiation energy fluency for the grating spatial frequency 52 lp/mm.

3.3.2. SLM with α-Si:C:H PC and ferroelectric LC

We have fabricated for these studies three specimens of SLM with the FLC layer thickness 2 μm (SLM 1), 5 μm (SLM 2) and 12 μm (SLM 3). Spontaneous polarization of FLC equaled 150..200 nC/cm^2, its helicon step was 0.2 μm and the tilt angle of the director θ_0 in smectic layer was 40 degrees. The refraction index modulation was obtained via S-effect.

Like in Sec.3.2.2, the SLM was fed by the superposed CW bias and sequence of rectangular voltage pulses. DE absolute value and its temporal behavior were

measured in two modes of grating recording. In the first one the gratings were recorded by the pulsed (20-30 ns) radiation at 0.54 μm, using the setup, described in it.3.1. In the second mode we have used the pulses of radiation with the wavelength 0.63 μm with the duration 50 ms and repetition rate 100 Hz. These pulses were cut off the CW emission of He-Ne laser, and reached the modulator synchronously with voltage pulses. The light pulses had the fronts 1 ms, light contrast ratio was not less than 1:20000.

In the course of our experiments we have varied the polarization of reading radiation, grating vector orientation with respect to the normal to the smectic layers, the recording energy fluency E, the bias V_b, the amplitude of controlling voltage pulses V_{pp} and the duration of the rectangular shaped pulses and the delay of the recording radiation pulse with respect to the forward front of the rectangular shaped pulse.

In the case of grating record with the use of the short light pulses the character of DE absolute value and temporal behavior dependence on the listed parameters was rather similar to that in the case of SLM with polymer PC and FLC (see Sec.3.2.2). Of course, the values of V_{pp} and V_b voltages, providing the maximal DE were another, as well as that of the grating reversibility without DE decrease. In the Fig.25 are shown the dependencies of DE vs.E, recorded for SLM 2 and SLM 3 for V_{pp} = 60 V and V_b = 45.5 V (SLM 2) and V_b = 48.5 V (SLM 3). The positive polarity of pulses was applied to FLC layer. The said bias values V_b provided realization of the optical memory mode (see Fig.16 and 17). Voltage pulse duration equaled 2 seconds, their repetition rate - 0.25 Hz and τ_0 - 5 ms. The gratings were read out by the non-polarized emission of the light emitting diode at 0.82 μm. The grating vector was perpendicular to smectic layers.

Significant DE drop with the spatial frequency increase from 50 to 100 lp/mm indicates the necessity to work over the reduce of the PC dark conductivity. Note,- however, that in this case the gratings' reversibility is to reduce. The discussed SLMs provided the reversibility of gratings record without the peak DE value drop for the repetition rates up to 6-8 Hz.

Higher reversibility of grating record was observed in the quasi-CW mode of SLM use. In the Fig.26 and Fig.27 are shown the dependencies of DE vs. recording radiation intensity fluency and vs. amplitude of pulses V_{pp} while recording the gratings with spatial frequency 85 lp/mm and the recording pulses repetition rate 100 Hz.

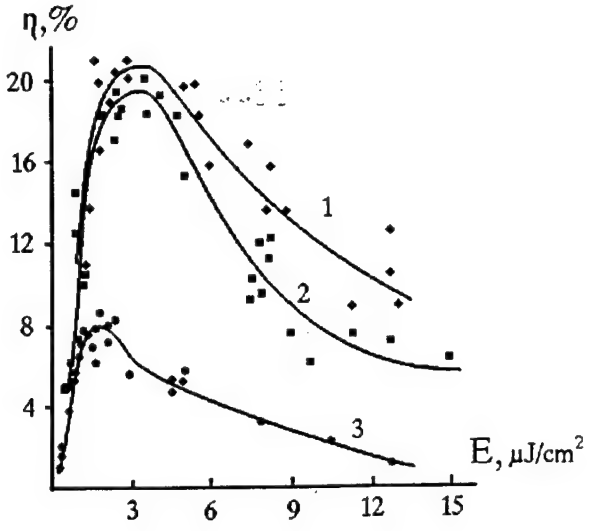

Fig.25. DE dependence on the recording radiation energy fluency for SLM 3 (curve 1) and SLM 2 (curves 2, 3); spatial frequency of grating 52 lp/mm (1, 2) and 100 lp/mm (3).

The dependencies in Fig.26 were taken for V_{pp} = 39 V and V_b = 29 V. The curves 1 and 2 illustrate the DE dependence on the voltage pulses polarity. The curve 1 corresponds to the case when positive pulse polarity was applied to LC layer and curve 2 - to PC layer. The dependencies in the Fig.27 were taken with the fixed recording radiation intensity fluency of 280 μW/cm^2. For each voltage V_{pp} the bias value V_b was chosen so as to realize the maximal DE. The curves 2 and 3 correspond to the cases when positive pulses were applied either to LC (curve 2) or PC (curve 3). Note that the dependence $V_b(V_{pp})$ is practically linear and practically does not depend on the FLC layer thickness and on the polarity of pulses V_{pp}

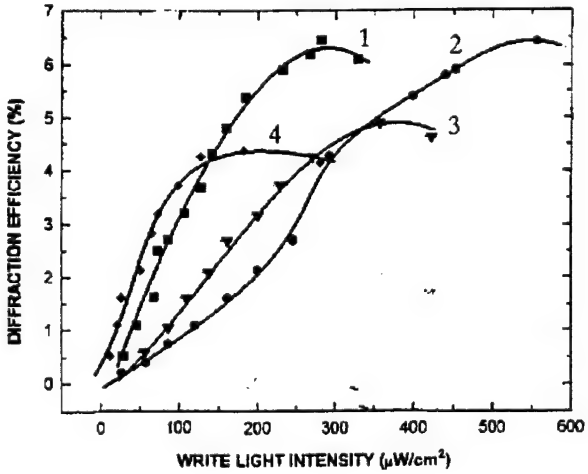

Fig.26. DE dependence on recording radiation intensity fluency for SLM with the FLC layer liquid of 2 μm (1, 2), 5 μm (3) and 12 μm (4).

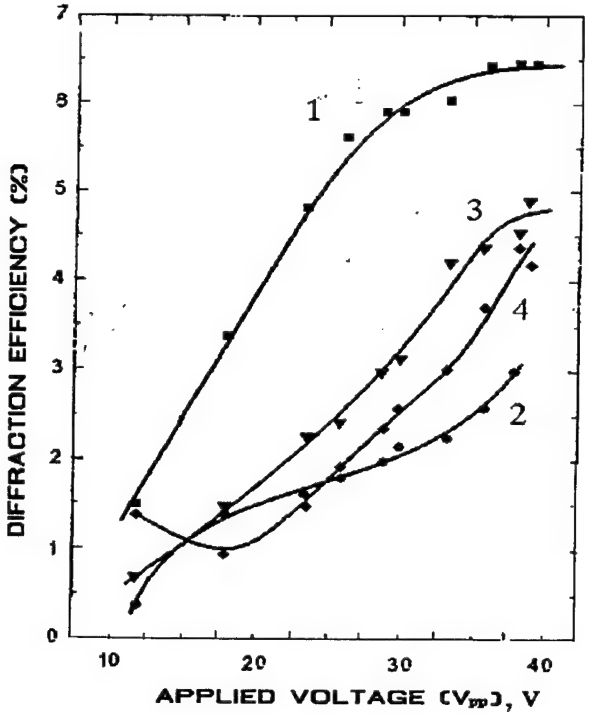

Fig.27. DE dependence on feeding pulses voltage for SLM with the FLC layer liquid of 2 μm (1), 5 μm (2, 3) and 12 μm (4).

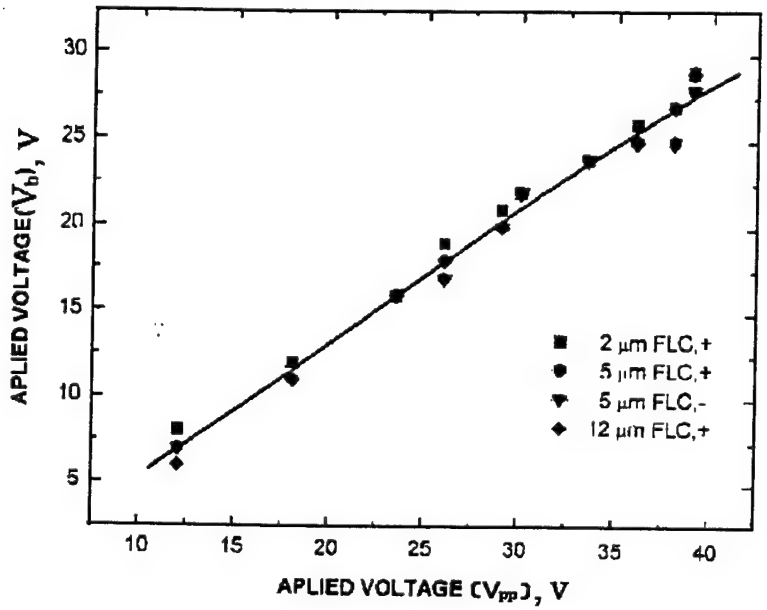

Fig.28 Mutual dependence of feeding voltages V_b vs. V_{pp}.

One can see from the given results that in quasi-CW (repetition rate 100 Hz) mode of gratings record the DE absolute value is much higher than one could expect on the base of the data on grating record by short pulses with the repetition period longer than the character time of transient processes. Most probably, this is the indication of some difference in the mechanism of the charge relief formation in two discussed modes of record.

3.4. Fidelity of correction for distortions in wide spectral range

The fidelity of image correction was studied with the use of SLM with the polymer PC. This type of SLM was chosen first of all due to the sufficiently high transparency of polymer layer in the visible range of spectrum and thus does not result in extra difficulties in spectral selectivity of image. In addition, this kind of SLM provided the sufficiently high DE for the grating with the spatial frequency ~100 lp/mm.

The studies were carried out with the dynamic holographic gratings with the fixed spatial carrier frequency 95 lp/mm. The various distorters were mounted in the signal beam. Small-scale distortions of the lens were simulated with the use of glass plates etched in hydrofluoric acid. For an example, in the Fig.29 the interferogram is shown of the "strongest" distorter of this kind, providing beam divergence of ~ 0.006 radian (FWHM). The Fresnel bi-prism was used for simulation of the local wedge-like distortions, which in practice can be caused, for example, by the mutual tilt of the primary mirror segments; the angular misalignment of "images" in our case was ~ 0.01 radian. We have used the tungsten wire of lamp, the sharp edge and the standard test object as the objects of imaging. The latter two kinds of test-objects provided the application of standard methods [36] of the quantitative evaluation of the correction fidelity and its dependence on the spectral range of imaging radiation.

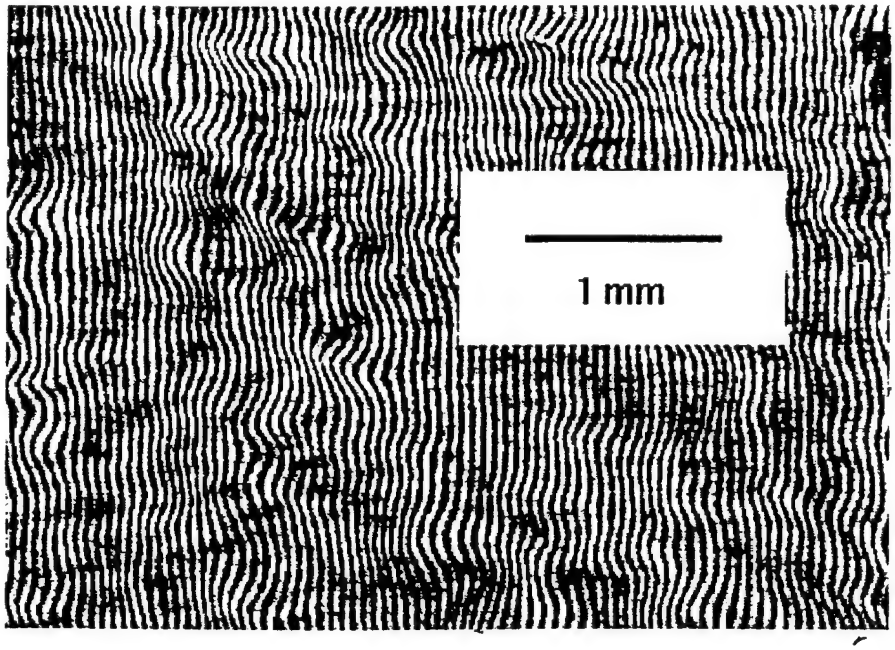

Fig.29. The part of interferogram of the distorting plate, providing beam divergence of 0.006 radian.

The following results were obtained with the NLC SLM:

- We have measured the frequency-contrast characteristics of the optical system under correction with the imitation of the small-scale scattering distorter with the angular divergence of ~ 0.006 radian. It was measured for the green range of spectrum (see filter transparency - curve 1 in the Fig.4), for the red range of spectrum (curve 2 in the Fig.4) and for the "white" light of tungsten lamp. In the Fig.30 the results are shown of this characteristic measuring as $K = \{I_{max} - I_{min}\} / \{I_{max} + I_{min}\}$. One can see from the Fig.30, that in the case of imaging in the green range of spectrum (the width of spectral range ~ 50 nm), whose maximum approximately coincides with the wavelength of laser radiation used for the hologram recording, the system performance is close to the diffraction limited. The use of "white" light also provides rather good quality of image. Significant deterioration of the image is observed only while imaging in red spectral band whose maximum is shifted in ~ 100 nm with respect to the recording wavelength. In the Fig.31 - 35 are shown the photographs of the standard test object, which confirm the above said.
- In the case of the wedge-like distortions the shift of imaging spectrum to the red range or use of "white" light the image was "expanded" due to incomplete compensation for the dynamic grating chromatism.

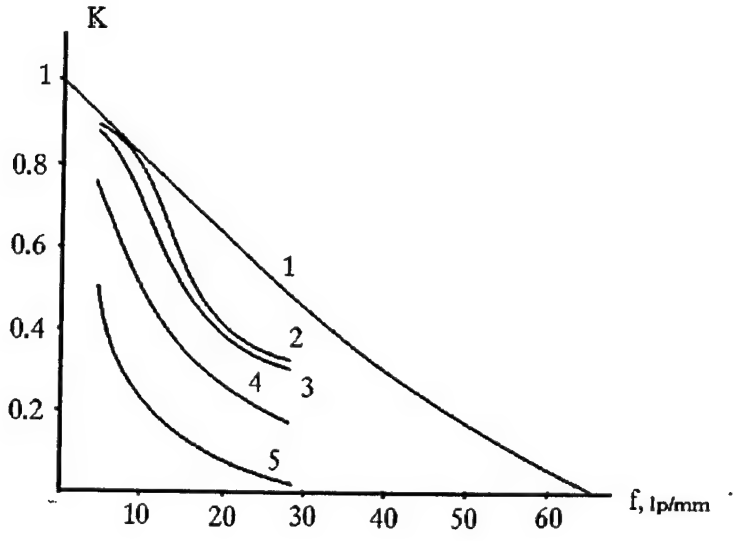

Fig.30. Frequency-contrast characteristics of the optical system under correction in the absence (curves 1, 2) and in the presence (curves 3, 4, 5) of small-scale distortions. Curve 1 - the ideal lens, curve 2 – optical system used in our experiment, 3 - correction in the green range of spectrum, 4 - correction in the "white" and 5 - light correction in the red range of spectrum.

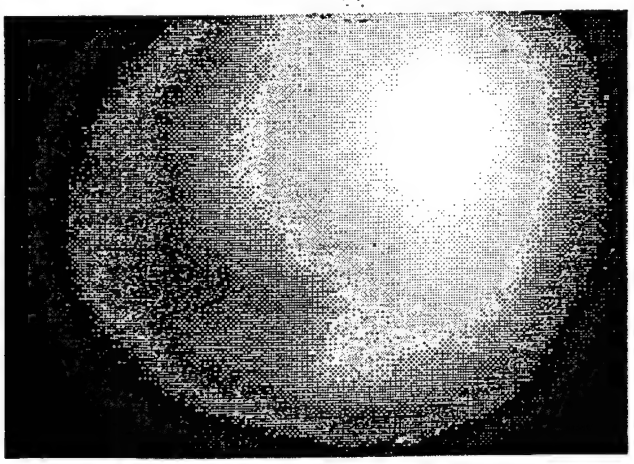

Fig.31. Image of standard test-object without correction for lens distortions.

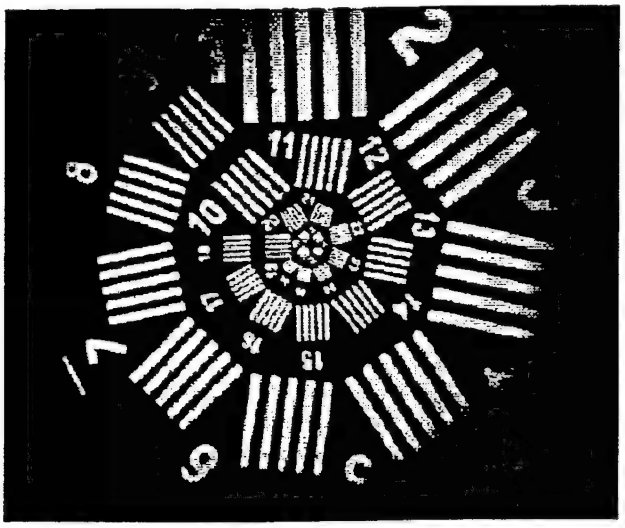

Fig.32. Image of test object in green light with correction for distortions.

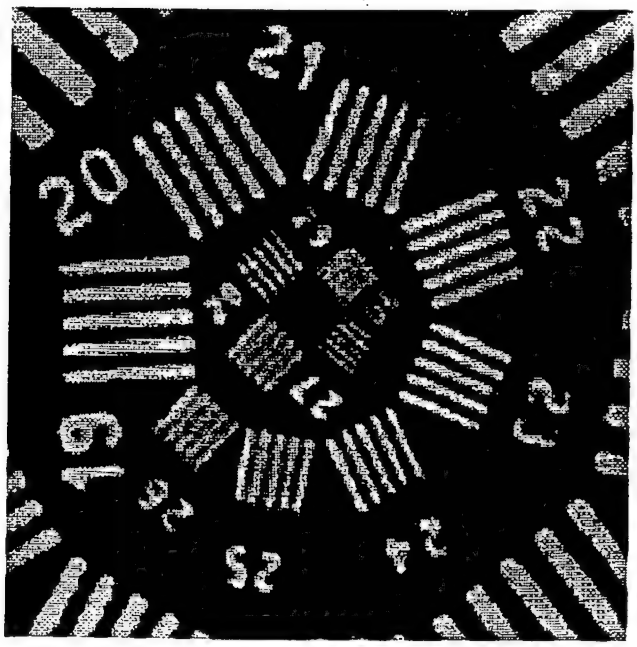

Fig.33. Central zone of standard test object image in green light with the correction for distortions.

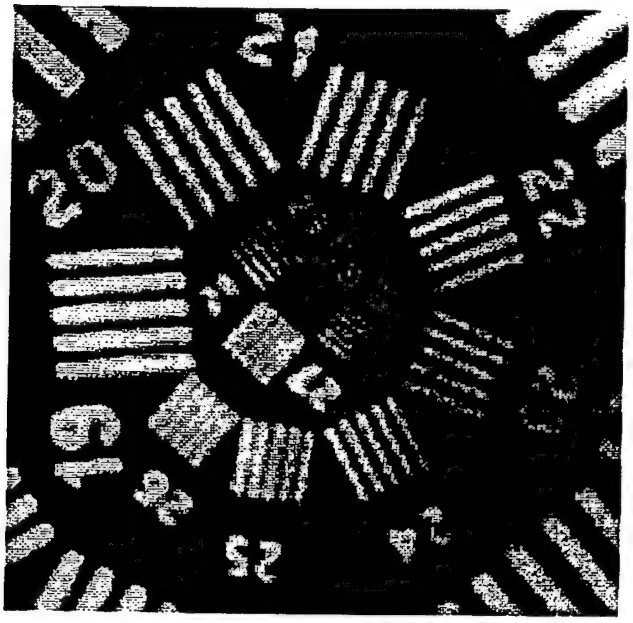

Fig.34. Central zone of standard test object image in "white" light with the correction for distortions.

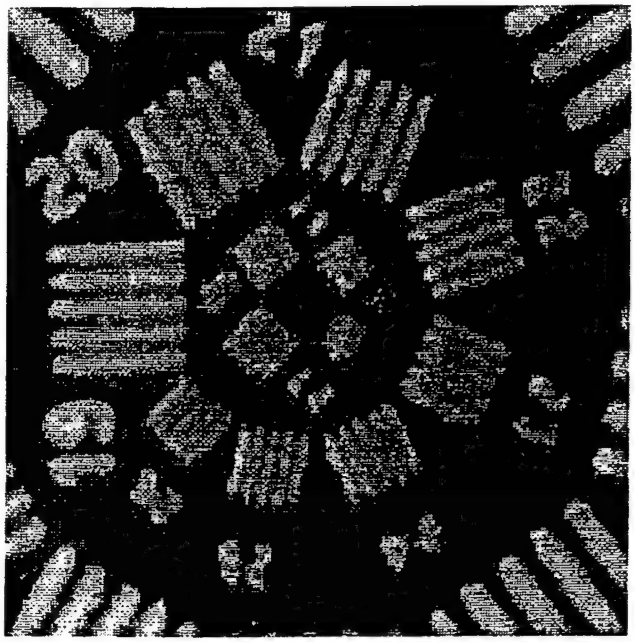

Fig.35. Central zone of standard test object image in red light with the correction for distortions.

- Additional information on the correction fidelity was got from the analysis of the photographs of the sharp edge (Fig.36, 37). One can see that in the case of spectral band shift with respect to the recording wavelength, and of the strong distortions of the probe beam, the wings in the edge spread function (ESF) are observed. These wings are responsible for the decrease of the complicated image contrast, and they are resulted from non-sufficient correction for the chromatism distortions. One can also see from these photographs that the point spread function (PSF) consists of two components: the narrow core, resulting of nearly diffraction limited performance of the OS, and of the wings, caused by the non-sufficient chromatic correction for the optical distortions. According to evaluations, in the absence of the distortions in the probe beam the image core contains ~ 65 % of total energy for reading out both in the green and in the red spectral ranges (Fig.36). Distortions of the probe beam by the etched plate with the distortions rate of 0.006 rad result, in the green range, in preservation of the core energy, while in the red range of spectrum it is reduced down to ~ 35% (Fig.37).

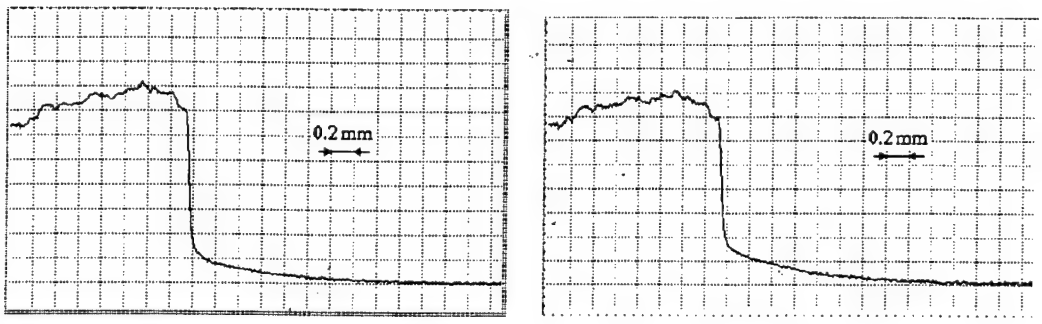

Fig.36. Reconstructed image of the sharp edge without distortions, reading out in green (a) and red (b) spectral bands (see Fig.4.).

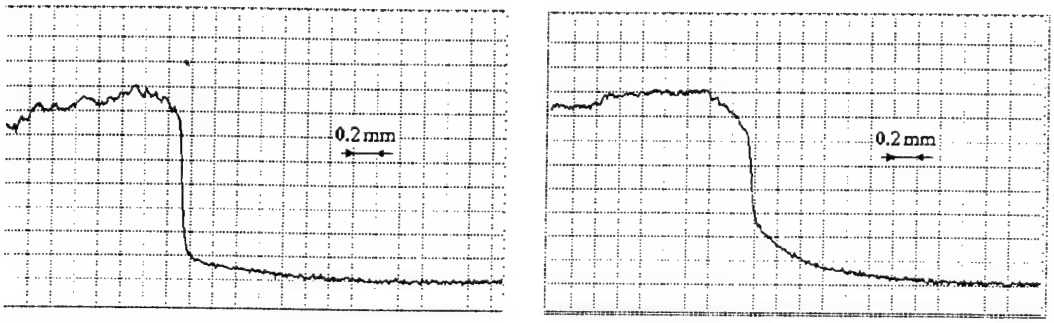

Fig.37. Reconstructed image of the sharp edge with distorter 0.006 rad. reading out in green (a) and red (b) spectral bands.

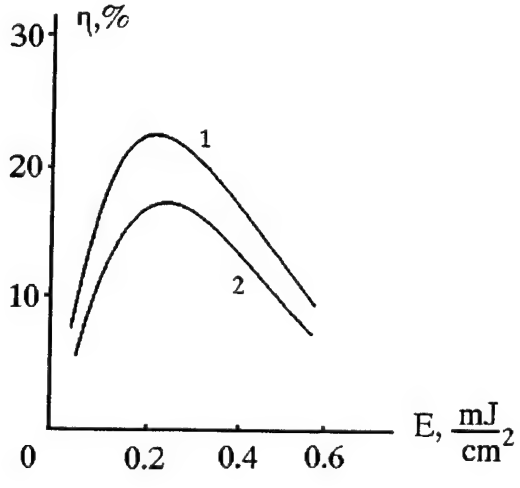

Fig.38. Peak values of DE vs. radiation energy fluency without distorter (1) and with the distorter 0.006 radian (2).

- It was found out that the influence of the small-scale distortions onto the absolute value of the hologram-correctors DE reveals itself for the etched glass distorters providing random divergence of more than 0.004-0.005 radian. These values are approximately in an order of magnitude smaller than the angular separation of neighboring orders of diffraction. Corresponding results, obtained by reading out by He-Ne laser radiation, are shown in the Fig.38.

In course of the experiments we have also tried the image correction with the use of SLM, based on the ferroelectric LC. Visual correction ability was not worse that in the case of nematic LC application. Image brightness, however, was much higher: in this case the radiation from thermal object is used much better, for the FLC SLM performance is almost polarization independent.

4. Conclusion

On the base of the studies performed we have shown that the application of the optically addressed SLM, based on the use of either polymer or a-Si_{1-x}:C_x:H photoconductor and of the either nematic or ferroelectric liquid crystal is prospective from the point of view of correction for optical elements distortions.

We have shown that the diffraction efficiency of SLM with FLC is almost independent to the polarization of the reading-out radiation. This is very important from the point of view of the discussed application of the device in the imaging optical systems. The reversibility and response time of such devices are determined by the properties of photoconductor.

The organic polymer photoconductors are interesting from the point of view of SLM design for the gratings with high (> 100 lp/mm) spatial frequency and high diffraction efficiency. In the reported study we have, in particular, realized the grating at 52 lp/mm with the diffraction efficiency of 35-40%, i.e. working quite nearby the theory limit for the thin (plain) holographic grating. Without any doubt the same results could have been realized in SLM with FLC, tested in this work, in the case of proper optimization of the FLC layer. The reversibility of gratings record in FLC SLM with polymer PC is limited by several Hz. Higher reversibility can be obtained by use of optical schematics of holograms recording (e.g. moving of record zone over the surface of a large SLM).

To our opinion, the photoconductor α-Si_{1-x}:C_x:H is more promising than the widely used now α-Si:H. Carbon content variation provides tuning of the dark conductivity of the layer, its sensitivity and spectral transparency across the wide range. So one can determine the proper trade-off between the spatial resolution and reversibility and to choose the PC sensitivity, corresponding to the problem under solution. In the reported work we have used this kind of α-Si_{1-x}:C_x:H PC of our own fabrication and with the definite carbon concentration, DE was realized about 20% and 6-8% for the gratings with the spatial frequency of 52 and 85-100 lp/mm correspondingly; reversibility of these elements was ~ 100 Hz. This result can definitely be improved by further optimization of carbon content and LC layer thickness and also by use of p-i-n structures; the possibility of such structures realization on the base of α-Si_{1-x}:C_x:H layers was shown in several papers, including ours.

The OA LC SLMs, which we have evaluated during the reported work, provide the correction for distortions in the imaging optical systems, working in the wide spectral range with the high optical quality. Application of such correctors makes it possible to realize the systems with the field of vision of at least one thousand diffraction limited angles, corresponding to the primary mirror (lens) aperture. The coefficient of distortions dumping can be as high as several dozens in the case of imaging in the visible range with the spectrum width of several dozen nanometers.

Further development of this work can be as follows.

Realization of high optical quality LC SLM with the stable and reliable parameters requires elaboration and creation of the technology module with the closed cycle of SLM fabrication. The parameters of the elements are to be optimized in accordance with this work result.

Special study can be devoted also to the elaboration of the advanced schematics of holograms recording. For example, the use of phase conjugation technique in the loop of the dynamic hologram record promises further improvement of the optical quality of the hologram corrector, which is difficult to be realized by means of just SLM fabrication technology improvement.

The corresponding work proposal is described in Appendix 1.

References

1. Yu.N.Denisuk, S.I.Soskin. Opt.Spektrosk., 1971, Vol.31, No.6, p.991-997, (in Russian).
2. Yu.N.Denisuk, S.I.Soskin. Opt.Spektrosk., 1972, Vol.33, No.5, p.994-996, (in Russian).
3. C.B.Burckhart, Bell Syst.Tech.Journal, 1966, Vol.45, p.1841.
4. J.Munch, R.Wuerker. Appl.Opt., 1989, Vol.28, No.7, p.1312-1317.
5. J.Munch, R.Wuerker, L.Héflinger. Appl.Opt., 1990, Vol.29, No.16, p.2440-2445.
6. Optical and infrared telescopes for the 1990. Ed. by N.Hewitt , Arisona, 1980.
7. N.V.Ryabova, D.N.Es'kov, A.P.Danilkin. Optical Journal, 1996, No.1, p.4-19. (in Russian).
8. M.A.Kramer, C.J.Wetterer, Ty Martinez. Appl.Opt., 1991, Vol.30, No.23, p.3319-3323.
9. H.Kogelnik. Bell Syst. Tech. J., 1965, Vol.44, p.2451-2455.
10. J.W.Goodman, W.H.Hantley, J.D.W.Jackson, M.Lehmann. Appl.Phys.Lett.,1966,Vol.8,p.311-313.
11. A.Yariv and T.L.Koch. Opt.Lett., 1982, Vol.7, p.113-115.
12. M.V.Vasil'ev, V.Yu.Venediktov, A.A.Leshchev, G.F.Pasmanik, V.G.Sidorovich. Izv.Akad.Nauk SSSR, Ser.Fiz., 1991, Vol.55, No.2, p.260-266. (in Russian).
13. A.A.Leshchev, V.G.Sidorovich, M.V.Vasil'ev, V.Yu.Venediktov, G.F.Pasmanik. International Journal of Nonlinear Optical Phys., 1994, Vol.3, No.1, p.89-100.
14. J.W.Goodman. Indroduction to Fourier Optics, McGraw-Hill Book-Company, 1968.
15. E.A.Vitrichenko. The methods of astronomic optics studying. Moscow, Nauka, 1980. (in Russian).
16. V.S.Myl'nikov, Photoconductivity of polymers, L. Khimiya, 1990, 240 p., (in Russian).
17. V.S.Myl'nikov, Optik. Zh., 1993, No.7, p.41-45, (in Russian).
18. M.A.Groznov, V.S.Myl'nikov, L.N.Soms, A.A.Tarasov, Zh.Tekh.Fiz., 1987, Vol .57, No.10, p.2041-2042, (in Russian).
19. N.V.Kamanina, L.N.Soms, A.A.Tarasov, Opt.Spektrosk., 1990, V.68, No.3, p.691-693, (in Russian).
20. V.A.Berenberg, N.V.Kamanina, L.N.Soms, Izv.Akad.Nauk SSSR, Ser.Fiz., 1991, Vol.55, No.2, p.236-238, (in Russian).
21. U.D.Dumarevski, N.F.Kovtonuk, F.I.Savin. Image Transformations by Semiconductor-Dielectric Structures. Moscow, Nauka, 1987, 176 p. (in Russian).
22. A.A.Vasil'ev, D.Cassasent, I.N.Kompanets, A.V.Parfenov, Spatial light modulators, Moscow, Radio i Svyaz, 1987, 320 p. (in Russian).
23. G.S.Chilaya, V.G.Chigrinov. Uspehi Fizicheskih Nauk, 1993, Vol.163, No.10, p.1-28 (in Russian).
24. I.Abdulhalim, G.Moddel. Mol. Cryst. Liq. Cryst., 1991, Vol.200, p.79-101.
25. N.A.Clark, S.T.Lagerwall. Appl. Phys. Lett. 1980, Vol. 36, No. 11, p.899-901.
26. M.F.Grebenkin, A.V.Ivashenko. Liquid crystal materials. Moscow, Khimiya, 1989, 288 p. (in Russian).
27. V.G.Chigrinov, V.A.Baykalov, E.P.Pozhidaev, L.M.Blinov, L.A.Beresnev, A.I.Allagulov. Zhurnal Eksperimentalnoi I Teoreticheskoi Fiziki, 1985, Vol.88, No.6, p.2015-2024,(in Russian).

28. G.Moddel, K.M.Johnson, W.Li, R.A.Rice, L.A.Pagano-Stauffer, M.A. Handschy. Appl. Phys. Lett., 1989, Vol. 55, No. 6, p. 537-539.
29. I.Abdulhalim, G.Moddel, K.M.Johnson. Appl. Phys. Lett., 1989, Vol.55, No.16, p.1603-1605.
30. P.R.Barbier, G.Moddel. Appl.Opt., 1992, Vol.31, No 20, p. 3898-3907.
31. K.Ahiyama, A.Takimoto, A.Ogivara, H.Ogawa. Jpn.J.Appl. Phys., 1993, Part 1, Vol. 32, p. 590.
32. N.A.Feoktistov, L.E.Morozova. Pisma v ZhTF, 1994, Vol.20, No.5, p.12-16, (in Russian).
33. N.L.Ivanova, N.A.Feoktistov, A.N.Chaika, A.P.Onokhov, A.B.Pevtsov. Mol. Cryst. Liq. Cryst., 1996, Vol. 282, p. 315-322.
34. K.Ahiyama, A.Takimoto, H.Ogawa. Appl.Opt., 1993, Vol.32, No.32, p. 6493-6500.
35. N.L.Ivanova, L.E.Morozova, A.P.Onokhov, A.B.Pevtsov, N.A.Feoktistov. Pisma v ZhTF, 1996, Vol.22, No.4, p.7-11, (in Russian).
36. G.V.Kreopalova, N.L.Lazareva, D.T.Puryev. Optical Measurements. Moscow, Mashinostroenie, 1987, 264 p. (in Russian)

Appendix 1. Optically Addressed Spatial Light Modulator Development for Compensated Imaging by Real-Time Holography (Proposals for the Statement of Work)

1. Background

In recent years, compensated imaging techniques have been studied as possible solutions to the problem of imaging with low-optical-quality primary mirrors. With relaxed requirements on the surface quality on the primary mirror, lightweight architectures for telescope system become feasible.

In order for the holographic compensation technique to become viable, a suitable hologram-recording medium must be developed. The hologram must meet requirements in the areas of speed, sensitivity, resolution, net optical efficiency, optical quality, and size. One of the best candidates for the hologram device is the optically addressed spatial light modulator (OASLM) generally consisting of a large area photoconductor and a liquid crystal layer situated between transparent electrodes. The beacon wavefront is interfered with a mutually coherent plane wave on the photoconductor surface. The intensity interferogram leads to modulation of the photoconductor conductivity creating an electric field distribution across the liquid crystal layer. Depending on the device configuration, this produces the effect of a phase or amplitude hologram.

To obtain the necessary characteristics of OASLM devices, a number of opportunities exist in varying the compositions of layers (modulating - including various ferroelectric liquid crystals using different optical effects; photosensitive - including non-organic and organic layers; orienting and conducting).

The results, described in the present Report indicate the prospective combinations of SLM, using ferroelectric liquid crystal with PC made of either polyimide (high spatial resolution) or silicon carbide (small response time and rather good resolution properties).

To realize these opportunities, and to provide the systematic search of the optimal OA SLM design and layers composition, the improvements of technology are needed.

2. Objective

The objective of this effort is to make technological improvements and optimization for OA SLM manufacturing process, as well as determining and measurements of characteristics of OA SLM responsible for the satisfactory operation as holographic correctors of large-size observation telescopes.

First, an emphasis shall be placed on development the technologies that provide sure and repeatable manufacturing of OASLM devices with the opportunities to vary the compositions of modulating, orienting, conductive and photosensitive layers in order to obtain necessary characteristics.

More specifically, the technological improvements will include the following:

- to provide the dust-less environment of manufacturing working place;
- to purchase the purest raw materials and to use them for photosensitive layers deposition;
- to make upgrades for technological equipment for films laser deposition, LC-filling and device assembling;
- to order and to manufacture the new compositions of ferroelectric LC;
- to upgrade the setup for OA SLM characterization, for quick and accurate measurements of OA SLM properties (resolution, net optical efficiency, and optical quality, as well as evaluation of OA SLM operation as correctors for real aberration in observational optical systems)

Second, an emphasis shall be placed on building devices with improved performance in the areas of resolution, net optical efficiency, and optical quality.

More specifically, the goal figures of OA SLM development are the simultaneous achievement of all of the following criteria:

- net optical efficiency: >20-25% with unpolarized read light
- resolution >60-70 lp/mm
- optical quality better then $\lambda/4$ over dia.25 mm
- refresh rate >100 Hz
- usable aperture >25 mm

3. Scope of work

This effort shall include the following:

- identification of limitations imposed by existing OASLM design and device;
- development of approaches to overcome these limitations:

- the choice, the purchase, the design, the manufacturing and the installation of specialized technological devices and the testing setup
- construction of devices implementing new approaches;
- the manufacturing the OASLM devices of various types using the equipment upgraded
- testing and characterization of new devices;
- delivery of new devices (5 (five) items)

4. Technical Tasks

4.1. Technology Improvements.

4.1.1. Dust-less environment of manufacturing working place: this must be done understanding that the impurities in LC layers deteriorate the optical quality of the device and make its behavior unpredictable;

4.1.2. Stabilization of response characteristics of OALSM: this will be done through the purchase the purest raw materials and using them for photosensitive layers deposition;

4.1.3. Maturing the technologies for components manufacturing and device assembling: this will be done by the upgrading of technological equipment for films laser deposition, LC-filling and device assembling;

4.2. OA SLM Design, Manufacturing, and Testing

4.2.1. OASLM modulating properties optimization: this will be done by the development of new compositions of ferroelectric LC specially designed to meet specific requirements of the application. These compositions will be ordered from LC researchers having established R&D connections with the Contractor, manufactured and used in OASLM devices;

4.2.2. Optimization of Net Optical Efficiency (NOE): The goal of this work is to produce a device with NOE close to the theoretical limit but not less then 20-25% for unpolarized light.

4.2.3. Optimization of Hologram Resolution: The goal of this work is to produce a device with NOE=(20-25)% at >60-70 lp/mm hologram fringe density.

4.2.4. Optimization of Hologram Speed: The goal of this work is to produce a device with NOE=(20-25)% at >60-70 lp/mm hologram fringe density operating at >100Hz.

4.2.5. Optimization Of Hologram Optical Quality: Since the purpose of the compensated imaging technique is to produce high-resolution images, it is a requirement that the OASLM does not introduce any aberrations. Consequently, all of the transmission and refractive optics must be better then $\lambda/4$ optical quality across the usable aperture dia.25 mm

4.2.6. Characterization Of Optically Addressed Spatial Light Modulator: The OASLM performance shall be characterized. The characterization shall include NOE vs. write-beam fringe density for the case of the plane-wave writing beams, diffraction efficiency vs. operating speed, interferometric characterization of the optical quality of the device. This will be done by the construction of a test setup aiming for quick and accurate measurements both of OASLM fundamental properties (such as resolution, net optical efficiency, and optical quality) and also of OASLM operation efficiency as the corrector for real aberrations in a test observational optical system.

4.2.7. OASLM manufacturing: 5 (five) samples of OASLMs must be manufactured, tested and characterized by the Contractor, and delivered to Customer.

5. Milestones & Deliverables.

5.1. Kickoff Meeting. A kickoff meeting shall be held within 30 days of the contract start date. This meeting will clarify any ambiguities and insure that both the contractor and customer have similar expectation of the effort. This meeting may take place at the contractor's facilities, or by electronic means.

5.2. Preliminary Design Review/Report. Within 60 days of the contract start date, the preliminary review/report must be done explaining the chosen approaches for the development of the technologies involved and device design based on sound physics and engineering principles.

5.3. Detailed Design Review/Report. Within four months of the contract start date, the Contractor shall provide the Customer with a detailed description of the OASLM device manufacturing technologies. The report shall include the explanation of anticipated technologies upgrades based on detailed physics and engineering analysis. The particular types of OA SLM to be delivered to Phillips Lab must be determined and specified at this stage. The report shall include anticipated performance of the device based on detailed physics and engineering analysis.

5.4. Manufacturing and Characterization of Improved OASLM (I) /Report. Within 7 months of the Contract start date, the Contractor shall provide the Customer with performance characterization data for various types of OASLMs produced within this stage of the Contract

5.5. Manufacturing and Characterization of Improved OASLM (II) /Report. Within 10 months of the Contract start date, the Contractor shall provide the Customer with performance characterization data for various types of OASLMs produced within this stage of the Contract

5.6. Final Report and Delivery of OASLM. At the end of 12 months after the Contract start date, the Contractor delivers the OASLM and final report to Customer. The final report shall include the OASLM design details, performance characterization, and operational instructions.

Appendix 2. Notes concerning LC SLM delivered to Customer

In course of the reported work there were fabricated and delivered to Customer two specimens of SLM with α-Si_{1-x}:C_x:H photoconductor, one with nematic LC and another with ferroelectric LC. Their properties are described in correspondingly Sec.3.3.1 (SLM 1) and Sec.3.3.2 (SLM 3) of this Report. In the SLM with NLC the director points onto the label "116", glued to the substratum. The orientation of smectic layers in SDLM with FLC can be determined from the indicatrise of the light scattered after voltage polarity switching.

Important notes!

- If in the course of work there would be necessary to switch the polarity of the voltage pulses, it is necessary first to switch off the bias voltage. Otherwise the combined action of bias and pulsed voltage can result in electric breakdown of the SLM.
- Mechanical fixation of SLM must not induce the mechanical stress in the direction, perpendicular to the SLM substratum. Otherwise the orientation of LC can be disturbed.